Higgs at Future e^+e^- Linear Collider

Satoru Yamashita

International Center for Elementary Particle Physics, University of Tokyo, Japan; CERN/EP/OPAL
(e-mail: Satoru.Yamashita@cern.ch)

Abstract

Higgs physics at the future e^+e^- linear collider, especially the measurements to be achieved in the phase-I at of the JLC project $\sqrt{s}$ =250–500 GeV, are reviewed. The key measurements and the problems to be solved before the experiment are discussed.

1 Introduction

The study of the Higgs particle [1], the only particle which has not been discovered so far in the Standard Model (SM), is the one of the keys to go beyond the SM. The Higgs bosons are very sensitive to the physics between the electro-weak and the Grand Unification (GUT) scale. The self-couplings of the Higgs easily diverge below the GUT ($\sim 10^{16}$ GeV) scale when we construct models beyond the SM, which leads to strong motivations to introduce the supersymmetry (SUSY). The existance of the light Higgs bosons expected in the SUSY models is to be clarified in experiments, which might open the next generation of the new physics paradigm in the coming 21st century.

Needless to say, the first priority of the Higgs study is to discover the Higgs boson(s). There are hopes that at least one of the Higgs can be discovered at currently running LEP-II [2], at Tevatron run-II [3] in the following years, or at LHC [4] which is expected to start from year 2005. The experiments at LEP-II can discover Higgs with mass of up to 105 GeV for the SM-like Higgs, and exclusion to 110 GeV. Tevatron run-II might exclude the mass region to 120 GeV. At forthcoming LHC, there are varieties of channels which have large discovery potential in wide range of the Higgs mass in the SM and the minimal supersymmetric extension of the standard model (MSSM). At the future e^+e^- linear collider such as JLC [5], the discovery potential is much higher than the experiments mentioned above. The discovery itself is really easy provided that we establish an accelerator with high luminosity of more than 10^{33} $cm^{-2}s^{-1}$ at the beam energy high enough to produce Higgs boson kinematically, and Higgs production cross-section similar to that of the SM Higgs. However the Higgs study does not mean just a discovery. The real Higgs physics starts after that. Profound knowledge on the structure of the fundamental interaction could come from precise measurements of the properties of the Higgs particle, such as cross-section and branching ratio of its decay. Through these measurements, our ultimate motivations of the Higgs studies are satisfied when we establish the Higgs mechanism and precise determination of the interaction strength with gauge bosons, Yukawa-coupling, and Higgs self-couplings. Such precise measurements can be done only by the next e^+e^- colliders. At LHC, the discovery of the Higgs boson(s) are considered to be feasible in many channels [4]. However, the huge background in the pp collisions such as QCD processes, and less constraints in the kinematics due to spectator quarks/gluons, make the Higgs detection very difficult, and only limited production channels and decay branch can be available for the Higgs detection and measurements. For instance, the light Higgs detection ($M_h \sim$120 GeV) could be done only with the $\gamma\gamma$ decay channel of the Higgs, of which the branching ratio is expected to be 10^{-3} level. In such experimental environment, it is very difficult to measure the properties of the Higgs particle precisely enough. Also there are many possible scenarios in such as next minimal supersymmetric extension of the Standard Model (NMSSM), to have a Higgs production cross-section much lower than that expected in the SM or MSSM. The e^+e^- collider gives us the unique opportunity to measure the cross-section and the branching ratio in percent order or less in its error. This precision is essential to determine the fundamental structure of the interaction in nature.

2 Higgs models: Where is the Higgs?

Where is the Higgs and how many Higgs? Higgs should exist, in order to satisfy the local gauge principle and finite mass of the weak gauge bosons and fermions. In the minimal SM framework, we assume only one Higgs boson. In this economic scenario, the direct lower mass bound of the Higgs is around 90 GeV at the 95 % confidence level (CL) from LEP-II experiments. The indirect measurements for the Higgs mass, via logarithmic contributions in the various electro-weak measurements performed at LEP/LSC/Tevatron, resulted in the SM Higgs mass upper bound of about 230 GeV at the 95 % CL.

As one knows the SM Higgs sector has various problematic issues inside such as the fine-tuning problem, which becomes one of the strong motivation for SUSY. In general, more than one Higgs doublet fields are necessary in SUSY models, which leads multi Higgs bosons as physical states. In the MSSM scenario, there exist two CP-even Higgs, h^0 and H^0, one CP-odd Higgs, A^0, and the charged Higgs, $H^{\pm}$. In the MSSM there are more stringent boundary for the upper limit of mass of h^0, the lightest CP-even Higgs. At the tree level, h^0 mass has to be lighter than Z^0 boson. Contribution from the loop effects by the top quark and scalar top quarks can extend the possible mass region [6], however it cannot exceed 150 GeV. Even in the next minimal extension of MSSM (NMSSM), with additional SU(2) singlet field, the upper mass boundary of about 140 GeV has been calculated by Y. Okada et al [7], provided that the Higgs coupling is finite up to GUT scale ($\sim 10^{16}$ GeV). This kind of discussion can be made also in the most general case [8], which assume the additional singlet and triplet fields with respect to MSSM. In this case the boundary is relaxed to be about 210 GeV. Hence

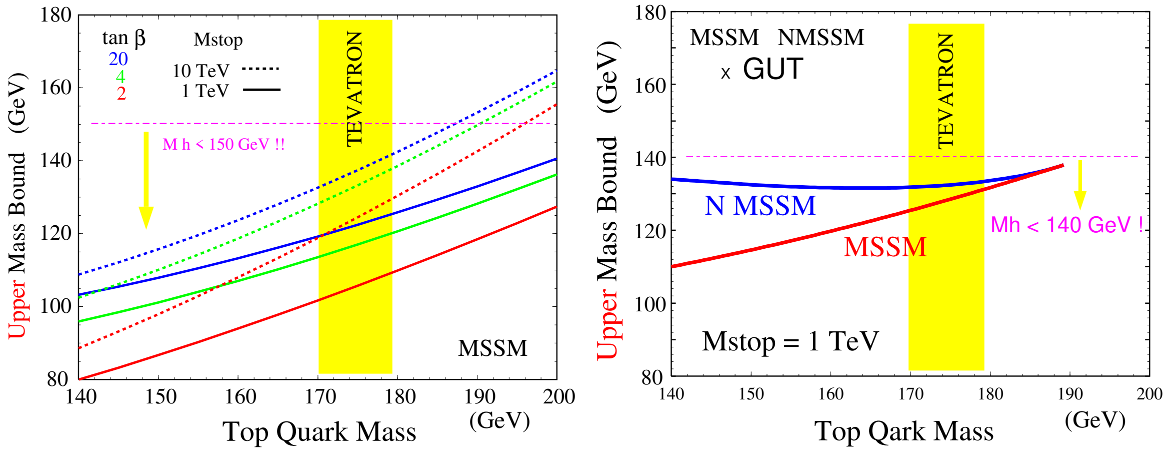

Figure 1: The upper bounds of the mass of the lightest CP-even Higgs boson in MSSM and NMSSM calculated by Y. Okada et al [7]. (Left) Upper bounds as a function of the top quark mass in the MSSM, with various MSSM parameters as shown in the plot. (Right) Upper bound for MSSM and NMSSM with additional constraints of the finite Higgs coupling up to GUT scale. The top quark mass measured at Tevatron is indicated by the grey bands.

at the first phase of JLC, apparently the target Higgs mass is from 100 GeV (just above the current LEP boundary) to 250 GeV. We may have a great opportunity to distinguish above these models of Higgs sectors and whole structure of nature only from the observed mass of the Higgs, as can be seen in the above mass boundaries.

3 Higgs production

In the e^+e^- collision, the CP-even Higgs (h^0), either in SM or SUSY models, can be produced via Higgs-strahlung (Bijorken) process, $e^+e^- \to Z^{0*} \to h^0Z^0$, and WW(ZZ)-fusion process, $e^+e^- \to \nu\bar{\nu}W^*W^* \to \nu\bar{\nu}h^0$ ($e^+e^- \to e^+e^-Z^*Z^* \to e^+e^-h^0$) as shown in Figure 2. The WW-fusion process becomes important at high energy. In the process, in principle, the kinematic boundary of the Higgs boson mass to be produced can be extended up to the e^+e^- centre-of-mass energy. This production has unique feature, which provide us the direct measurement of the coupling of the Higgs with W-boson. Note that the inferference between $h^0Z^0 \to h^0\nu\bar{\nu}$ and the WW-fusion process is large as seen in Fig. 3.

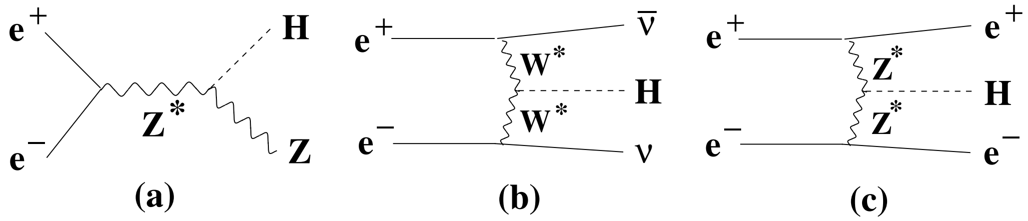

Figure 2: Diagrams of CP-even higgs production expected at JLC phase-I in (a) Higgs-strahlung (Bijorken) h^0Z^0 production, (b) WW-fusion and (c) ZZ-fusion process.

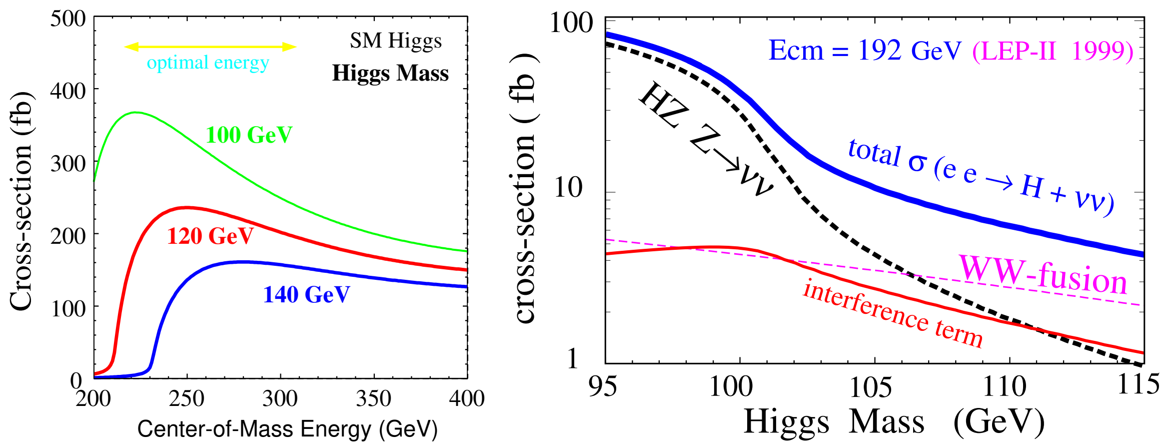

Figure 3: Production cross-section of the SM Higgs. (Left) The h^0Z^0 production cross-section for 100–140 GeV SM Higgs as a function of the centre-of-mass energy. (Right) The cross-section of the $e^+e^- \to \nu\bar{\nu}H^0$ process at $\sqrt{s} = 192$ GeV (LEP-II energy) as a function of Higgs boson mass, taken from Ref. [9]. The effect of the interference term is also shown.

In the SM Higgs, the production cross-section is completely determined for a given Higgs mass. No free parameter exists except for Higgs mass itself. Figure 3 shows the production cross-section. With a naive calculation we have approximately 10^5 Higgs events in 5 years for 120 GeV Higgs if we have the luminosity of 10^{34} $\mathrm{cm}^{-2}\mathrm{s}^{-1}$, with 10^7 seconds running per year.

For MSSM, the production cross-section of the h^0Z^0 process $\sigma_{\mathrm{hZ}}^{\mathrm{MSSM}}$ can be written as $\sigma_{\mathrm{hZ}}^{\mathrm{MSSM}} = \sin^2(\beta-\alpha) \times \sigma_{\mathrm{HZ}}^{\mathrm{SM}}$, where $\sigma_{\mathrm{HZ}}^{\mathrm{SM}}$ is the SM Higgs cross-section. The β is defined by $\tan\beta = v_1/v_2$, the ratio of the vacuum expectation values of two Higgs doublets. The α is the mixing angle of the two CP-even Higgs states. Note that the α and β are related in the MSSM in terms of CP-odd Higgs boson (A^0) mass and other SUSY parameters. In more general SUSY Higgs models such as NMSSM, the cross-section depends on more parameters. However, there exist absolute lower limits of the cross-section ($\sigma_{\mathrm{minimum}}$). Figure 4 shows the $\sigma_{\mathrm{minimum}}$ as a function of centre-of-mass energy of e^+e^- collision for the NMSSM, taken from Ref. [7], which are valid also for the MSSM Higgs.

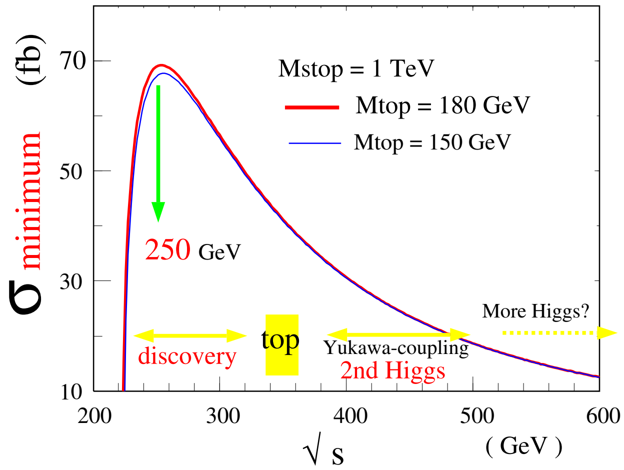

Figure 4: The minimum cross-section of the CP-even higgs production in the NMSSM calculated by Y. Okada et al [7]. The two lines correspond to the top quark mass of 150 and 180 GeV.

The other Higgs expected in the multi Higgs models such as MSSM might also be discovered even in the first phase of JLC project at $\sqrt{s}$ lower than 500 GeV. For MSSM (or general two Higgs doublets scenario), there is an additional important channel, which is $e^+e^-\to A^0h^0$. However, if we stick to the MSSM, the production cross-section of the A^0h^0 process is expected to be too small to be observed, if the h^0 mass exceed 110 GeV, where LEP-II sensitivity ends. The heavier Higgs such as A^0 and H^0 would be the essential subjects to be investigated at the second phase of the JLC at $\sqrt{s}$ higher than 500 GeV.

In the second phase, the important measurement would be A^0 (H^0) production radiated off the b quark or top quark, for example $e^+e^-\to b\bar{b}\to b\bar{b}A^0$, via Yukawa-coupling. Also other channels with multi-Higgs production could be observed via Higgs self-coupling. The strategy and scenario at the next step depend on the results of the first phase.

4 Higgs Decay

The decay branching ratio of the SM Higgs is shown in figure 5. The Higgs boson couples to mass of the particle (coupling determines mass of the particle via Higgs mechanism). If the Higgs is of the SM like, the dominant decay branch is $b\bar{b}$ for Higgs mass of less than 130 GeV. However, once the decay channel into W pair open, the most of the Higgs is expected to decay to W pair. The decay of the MSSM Higgs depends also on α and β. For the target mass region between 100 and 140 GeV where we expect the lightest Higgs in MSSM and NMSSM, the $b\bar{b}$ branch dominates in wide range of the parameter space. A good b-flavour tagging is the essential technique to discover and measure the Higgs boson.

5 Important Measurements at the Phase-I

As we discussed, the essential measurements of the Higgs is the coupling to other particles and Higgs particle itself. These can be achieved by the precise measurements of the Higgs production cross-section and the decay branching ratio. The key measurements at the first phase of the JLC would be as follows;

- Mass of the Higgs.
- Cross-section measurements in Z^0h^0 and WW-fusion channels.
- Branching ratio to $b\bar{b}$ ($Br(h^0\to b\bar{b})$).
- $Br(h^0\to W^+W^-)$.
- $Br(h^0\to\tau^+\tau^-)/Br(h^0\to b\bar{b})$.
- $Br(h^0\to c\bar{c}(+gg))/Br(h^0\to b\bar{b})$.

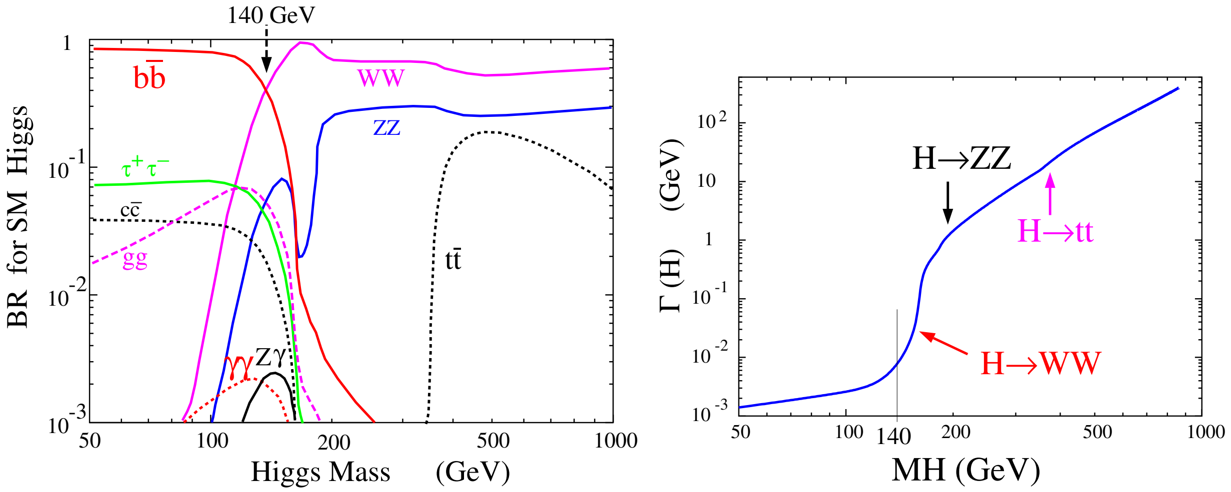

Figure 5: The branching ratio (Left) and the total decay width (Right) of the SM Higgs as functions of the Higgs mass.

The measured values are combined to study the following physics issues;

- Coupling of Higgs with weak bosons.
- Natural width of the Higgs.
- Yukawa-coupling strength to fermions.
- Discriminate SM or SUSY.
- If SUSY, indirectly measure other Higgs masses.

The cross-section measurement of the Z^0h^0 production and WW-fusion process enable us to measure the coupling between Higgs and the weak gauge bosons. Also the relative strength of the coupling with fermions are determined by the measurements of the Higgs decay branching. The absolute strength of the Yukawa-couplings are derived with combination of the cross-section measurement and the Br-measurement to $f\bar{f}$ and W^+W^- (or Z^0Z^0). These results would judge whether we live in the SM-like nature or in SUSY world.

5.1 Mass measurements

The Higgs boson mass is the fundamental value which might give us information up to GUT scale as we discussed above. Just knowing the Higgs mass with accuracy of 5 GeV, we might be able to select the possible models of the Lagrangian. However the very precise measurement of the Higgs mass with an accuracy of 100 MeV is necessary in order to obtain fruitful results from the other measurements such as branching ratio. Because the Higgs branching ratio is the very strong function of the Higgs mass, as we have discussed above. For these purpose, precise calibration of the detector and beam energy measurement are essential. Calibration runs at Z^0 pole [11] might be very helpful.

5.2 Cross-section measurements

As we discussed, the cross-section measurements of the Z^0h^0 (and WW-fusion) process mean the direct determination of the coupling between Higgs and Z^0 (and W bosons). In the Z^0h^0 production, the event topologies are categorised by the final state of the associated Z^0 boson, namely $q\bar{q}$, $\tau^+\tau^-$, $\nu\bar{\nu}$, e^+e^- and $\mu^+\mu^-$. In order to measure the cross-section independently of the Higgs decay branching, the simplest way is to use $e^+e^-\to Z^0h^0\to\mu^+\mu^-h^0$ channel in the recoil mass distribution of the muon pairs. We add the statistics with electron channel which include small contribution from the ZZ-fusion.

These leptonic channels have small branching compared to all Z^0h^0 production due to only 3 % of the branching from Z^0 to each lepton flavour. Hence the inclusion of the other channels is helpful. Once we measure the branching ratio to $b\bar{b}$ or W^+W^-, the other channel can also be used to determine the cross-section more precisely. In this case, however, the precision of the cross-section measurement is determined by that of the Br-measurements.

5.3 Branching ratio measurements

The measurements of the branching ratio (Br-measurement) of the Higgs is one of the keys to distinguish the SM and other models such as SUSY. Once we determine the Higgs mass, the branching ratio of the SM Higgs is completely determined by the known SM parameters. On the other hand, for SUSY Higgs, the branching can be affected by other SUSY parameters such as A^0 mass or $\tan\beta$, which result in the different branching ratio from the SM case. When we assume heavy ($\sim$ 2 TeV) mass for A^0 and other SUSY particles, the branching ratios in MSSM are very similar to those of the SM by the decoupling theorem. There are a lot of Br-measurements. Of these the most interesting are the Br-measurement of Higgs decaying into $b\bar{b}$, $\tau^+\tau^-$ and W^+W^-.

When we combine the $\mathrm{Br}(h^0 \to W^+W^-)$ with the cross-section measurement, the total width of the Higgs can be deduced. The absolute coupling of Higgs and W boson can be determined by the cross-section measurement either of Z^0h^0 production with SU(2)×U(1) coupling assumed, or of the WW-fusion process. The partial width of the Higgs to WW, $\Gamma_{h^0 \to W^+W^-}$, is calculable from the coupling strength obtained by the cross-section measurement. It can be written as

$$\Gamma_{h^0 \to W^+W^-} = \Gamma^{SM}_{h^0 \to W^+W^-} \times \frac{\sigma_{h^0Z^0}}{\sigma^{SM}_{h^0Z^0}} \quad , \tag{1}$$

where $\Gamma^{SM}_{h^0 \to W^+W^-}$ is the partial width of the $h^0 \to W^+W^-$ in the SM, $\sigma_{h^0Z^0}$ is the production cross-section obtained in the experiment, and the $\sigma^{SM}_{h^0Z^0}$ is that for the SM. Finally the total width of the Higgs Γ_{h^0} is calculated as

$$\Gamma_{h^0} = \frac{\Gamma_{h^0 \to W^+W^-}}{\mathrm{Br}(h^0 \to W^+W^-)} = \Gamma^{SM}_{h^0} \times \frac{\mathrm{Br}^{SM}(h^0 \to W^+W^-)}{\mathrm{Br}(h^0 \to W^+W^-)} \times \frac{\sigma_{h^0Z^0}}{\sigma^{SM}_{h^0Z^0}} \quad , \tag{2}$$

where $\Gamma^{SM}_{h^0}$ is the total width for the SM Higgs. In a similar mannar, the absolute strength of the Yukawa-couplings of the Higgs boson to fermions can be deduced in a model independent fashon, using the relative branching ratio $\mathrm{Br}(h^0 \to f\bar{f})/\mathrm{Br}(h^0 \to W^+W^-)$ together with the measured cross-section.

The ratio $\mathrm{Br}(h^0 \to \tau^+\tau^-)/\mathrm{Br}(h^0 \to b\bar{b})$ is also the one of the essential measurements. In SM, various SUSY, and also in more general of type-II in two Higgs doublets model, an universal coupling to the charged lepton and down-type quarks are assumed. While the different absolute values of the Yukawa-coupling strength are expected in models, the ratio $\mathrm{Br}(h^0 \to \tau^+\tau^-)/\mathrm{Br}(h^0 \to b\bar{b})$ is the same in the SM and type-II models. On the other hand, if we assume the Type-II coupling like SM or MSSM, the measurement serves as the precise measurement of the running b-quark mass at the Higgs mass.

The measurements of $\mathrm{Br}(h^0 \to c\bar{c})/\mathrm{Br}(h^0 \to b\bar{b})$, $\mathrm{Br}(h^0 \to gg)/\mathrm{Br}(h^0 \to b\bar{b})$ or $\mathrm{Br}(h^0 \to c\bar{c}+gg)/\mathrm{Br}(h^0 \to b\bar{b})$ have interesting feature. The gluonic decay occurs mainly due to the top quark loop, and it has similar SUSY-parameter dependence to the Higgs decay to c-quarks. J. Kamoshita et al [12] calculated the effects of the SUSY-parameters in MSSM as shown in Fig 6.

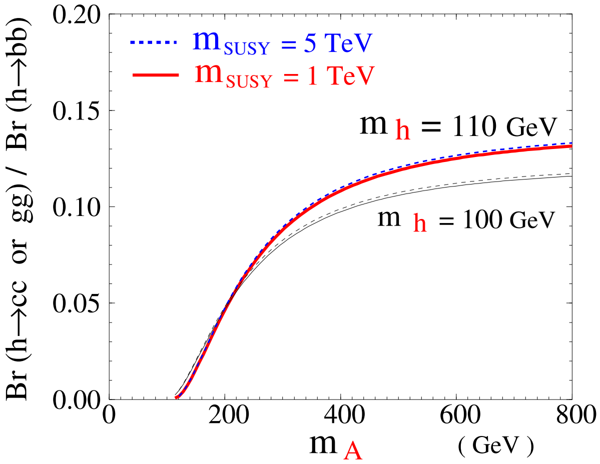

Figure 6: The ratio $Br(h^0 \to c\bar{c} + gg)/Br(h^0 \to b\bar{b})$ predicted by J. Kamoshita et al [12] in MSSM, as a function of the mass of the CP-odd Higgs (A^0).

The expected value of $Br(h^0 \to c\bar{c} + gg)/Br(h^0 \to b\bar{b})$ for 110 GeV Higgs in the SM is about 15 %. The ratios are sensitive to A^0 mass in MSSM, with little dependence on other SUSY parameters such as scalar top mass. The figure indicates that we can discriminate SM and MSSM in case A^0 mass less than 500 GeV with the Br-measurement accuracy of 10 %. Preliminary expectation of the experimental sensitivity of the Br-measurement are found in Ref [13] and [14]. However one should note that the line in the figure have, in relative, about 10 % ambiguity due to the uncertainty of the c-quark mass and strong coupling constant which affect the gluon radiation rate, while we expect more precise measurement of the α_s at JLC. Theoretical improvements are awaited.

6 Physics Background, Flavour Tagging, and Model Detectors

Here we review the physics background of the Higgs measurement, heavy flavour tagging such as b-tagging which is crutial in the Higgs studies, and preliminary results of the simulation studies with model detectors.

6.1 Physics backgrounds

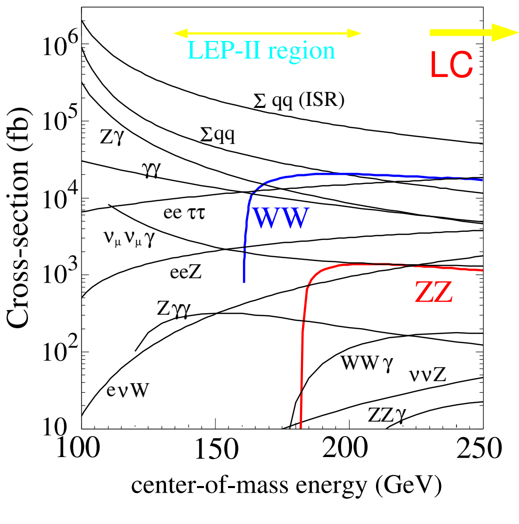

Figure 7: Cross-section of the physics background as a function of centre-of-mass energy at LEP-II region and above.

Bkg process	cross-section
$q\bar{q}(\gamma)$	35 pb
W^+W^-	17 pb
Z^0Z^0	1.0 pb
$We\nu$	2.0 pb
$Z^0e^+e^-$	1.2 pb

Table 1: The cross-section for background processes of the Higgs hunting at $\sqrt{s}$ = 300 GeV. The signal cross-section of the process $e^+e^- \to h^0Z^0$ is about 0.2 pb for the SM Higgs with mass of 120 GeV.

Table 1 shows the cross-section of the SM background processes at $\sqrt{s}$=300 GeV. The $q\bar{q}(\gamma)$ background is relatively easy to be reduced by analyses in the event topology. The most severe background is the W pair production. In case Higgs boson mass close to Z^0 mass, the $e^+e^- \to Z^0Z^0$ process with heavy flavour or tau lepton in the final states could be irreducible backgrounds. Note that the physics background can be strongly suppressed by the polarised beam option [10], which is one of the big advantages of the linear collider. The situation is much better than LHC where several order of magnitude higher background level is expected. However our ultimate purpose of the Higgs study is not only the Higgs discovery, but also to measure the Higgs properties precisely, in order to determine the direction of the future physics. The requirements of the purity and accuracy are far beyond those at LHC.

6.2 Heavy Flavour Tagging

As we have discussed, if the Higgs boson has mass of less than 140 GeV, the dominant decay mode is expected to be $b\bar{b}$. Hence the b-flavour tagging is the essential technique in the Higgs study. Figure 8 shows a schematic view of the cascade decay of the b-hadron. The b-hadron tends to decay sequentially to c-hadron and to hadrons with strangeness. The lifetime of the b-hadron is long enough ($\beta\gamma c\tau \sim$3–5 mm) to be observed as a displaced vertex in the detector.

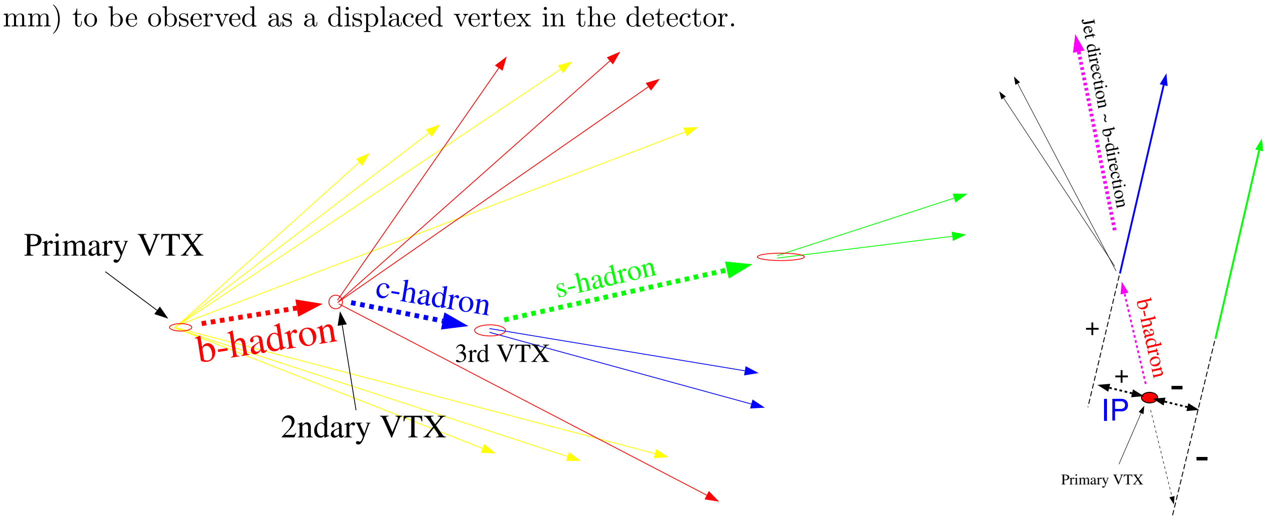

Figure 8: Schematic view of the cascade decay of the b-hadron (Left) and the scheme of the definition of the impact parameters (Right) for the heavy-flavour tagging.

One defines the impact parameter of the tracks as shown in figure 8. Tracks are extrapolated to the beam interaction region, and the displacements are measured from the extraporated position to the event production points (primary vertex). The primary vertex resolution at JLC is expected to be much better than that of LEP, since the beam size of less than μm at JLC can be used as constraints of the primary vertex fitting. Several properties of the $b\bar{b}$ decay of the Higgs signal in terms of the decay length of the b-hadron originating from Higgs decay and so on, can be seen in Figure 9. The dominant part of the charged particle from the b-hadron decay have its momentum of less than 2 GeV. Hence the low momentum track is important for the efficient Higgs tagging. One can see, to establish the Higgs tagging with more than 80 % for $b\bar{b}$ decay with reasonable purity of signal against background process, predominantly WW production, we need to tag the secondary vertex for that with decay length less than 1 mm. There are many methods for efficient b-tagging developed and used in the existing experiments. One reconstruct the secondary vertex or vertices representing the sequential decay of the b-hadron to c-quark and lighter flavour. The other way is using the displaced track with respect to the event primary vertex. This method does not require actual reconstruction of the secondary vertex, hence it has high efficiency but with lower purity. Kinematics of the jet is also the one of the discriminatory of the b-hadron against lighter flavours. The b-hadron tends to decay with large multiplicity and large jet invariant mass due to heavy mass of the b-quark. SLD experiment at SLC extensively uses the combined information of the vertex decay length and its mass (SLD mass tagging). At LEP, sophisticated methods combining several discriminant variables are used. For example OPAL experiment uses lifetime tagging based on an artificial-neural-network combined with high p_t lepton tagging and jet kinematics. The feature of the tagging methods can be seen in Fig. 10.

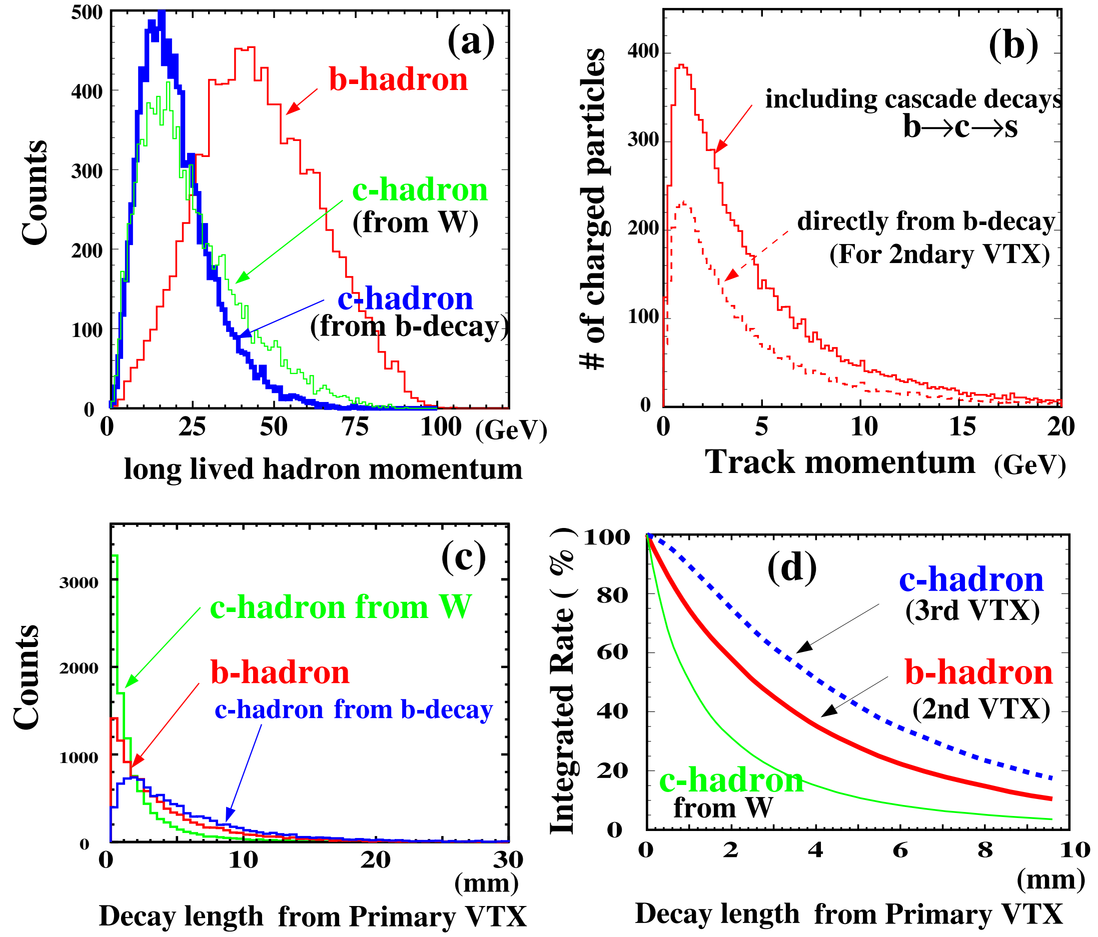

Figure 9: Properties of the b and c-hadrons and decay products from Higgs boson and background W pair production: (a) The momentum distribution of the heavy-flavour hadrons. (b) Distributions of the track momentum originating the b-hadron decay. (c) Distributions of decay length (the distance from the event production point to the decay point. (d) Rate (tagging efficiency) in integration of events as a function of the cut position of the decay length from the event production point.

6.3 Study with OPAL detector at LEP

One of the realistic estimates of the background effects for Higgs hunt would be made by a simulation study of existing detector. We have studied the potential of the Higgs hunt with full simulation code of the OPAL detector at LEP. The centre-of-mass energy of 250 GeV and the production of the SM Higgs with 120 GeV mass is assumed. The tagging of the Higgs event uses the existing OPAL energy-flow and b-tagging algorithms of our own which are actually used in the OPAL LEP-II Higgs search now. The simulation is known to model the detector effect precisely enough, hence reliable, although the expected performance of the detector at JLC is expected to be much better than that of the detectors at LEP. Hence one should take the results obtained here just as an indication of the lower limit of the sensitivity. Table 2 shows the signal selection efficiencies obtained by I. Nakamura et al. The figure 11 shows the reconstructed mass distribution for the events after selection. The effective cross-section after the selection is 28.2 fb for the signal in the mass window indicated in Figure 11. The background has been reduced to 7.2 fb after the selection. At a glance, even with the integrated luminosity of 1 fb^{-1}, which corresponds to only about one day running of JLC, we can discover Higgs easily, even with the performance of the detector currently running at LEP. This is encouraging result. However, in order to achieve the purpose of our precise measurements at JLC, a detector much better than that of present experiments are to be required.

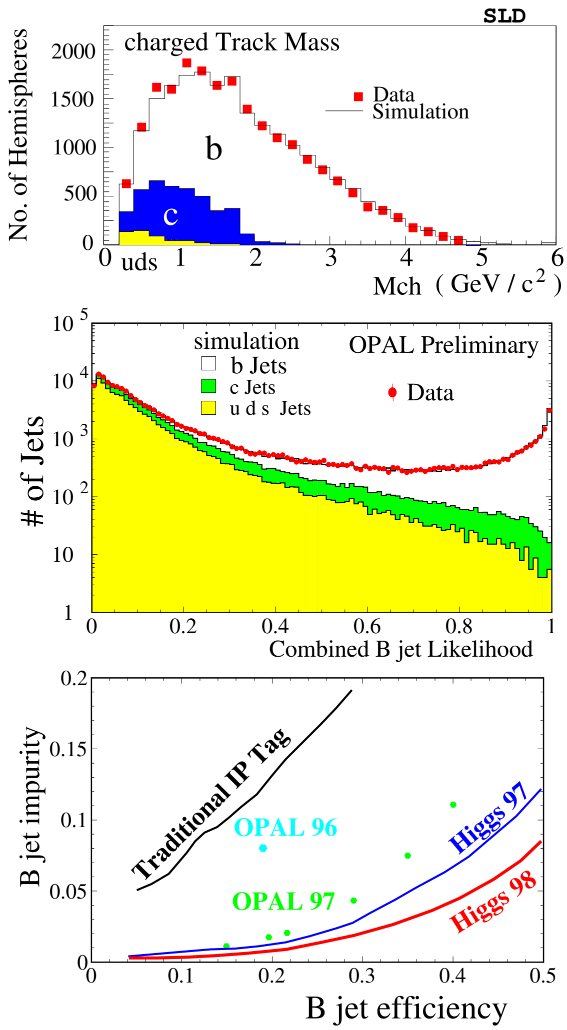

Figure 10: (Top) Distribution of the invariant mass of the charged tracks from the secondary vertex, used in SLD experiment at SLC (SLD mass tag) in R_b measurement. (Middle) Distribution of the b-flavour discriminant variable $\mathcal{B}$ from the b-tagging algorithm used in OPAL experiment for Higgs search. The data in Z^0 pole run are compared to the simulation. (Bottom) The performance of the OPAL b-tagging. The improvements by combinations of multi-variables are shown. The line indicated as "traditional IP tag" is just with the impact parameter. "OPAL 96–97" are just with the secondary vertex tagging.

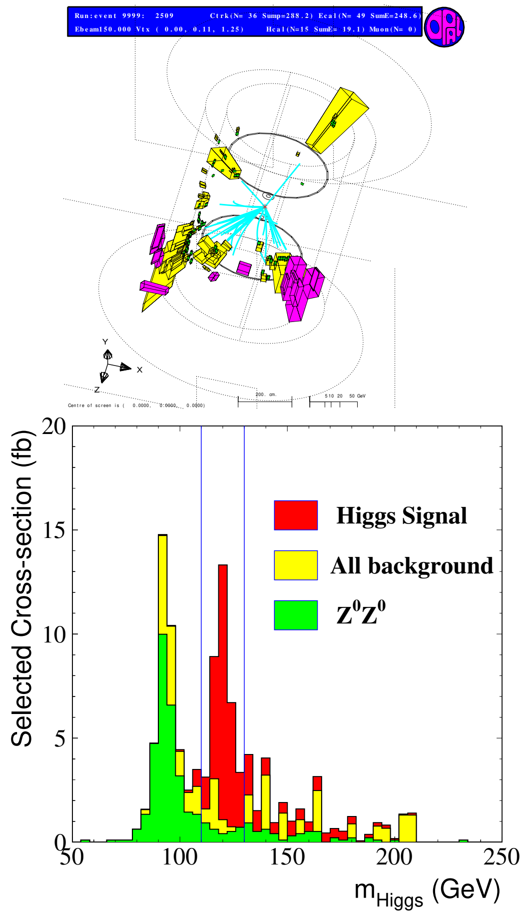

Figure 11: Demonstration of Higgs hunt with OPAL detector at $\sqrt{s} = 250$ GeV.

Channel	Higgs selection efficiency (%)	
	All mass	in mass window
$q\bar{q}$H	21	15
$\nu\bar{\nu}$H	13	9
$\mu^+\mu^-$H	50	40
e$^+$e$^-$H	49	39
total	20	14

Table 2: The selection efficiencies for the signal process e$^+$e$^-$$\rightarrow$h^{0}Z^0 for Higgs mass of 120 GeV at $\sqrt{s} = 250$ GeV, obtained with the full simulation of the OPAL detector at LEP. The efficiencies are shown separately without reconstructed mass cut and after the mass selection between 110 and 130 GeV.

6.4 JLC-I detector

The technical key points of the Higgs measurement can be summarised as follows;

- Good energy measurement of charged track, neutral particles, and jets, in order to reconstruct Higgs boson mass.
- Precise positioning of the primary and the secondary vertices in order to tag the b-quark and c-quark from Higgs decay.
- Good hermeticity of the detector. It is essential especially for the neutrino channel, $e^+e^- \to h^0 \nu\bar{\nu}$, in $e^+e^- \to h^0 Z^0$ and WW-fusion ($e^+e^- \to \nu\bar{\nu} W^{+*} W^{-*} \to \nu\bar{\nu} h^0$) processes.
- Particle Identification especially for leptons. The τ-identification performance is the one of the keys of the Higgs study.

A model detector, JLC-I, has been designed by JLC group. Current detector design is shown in Fig 12. The details can be found elsewhere [15]. The detector consists of the interaction region (IR) with a detector mask, surrounded by two to three layers of silicon base CCD vertex detector (SI-VDET), central drift chamber (CDC) of mini-jet-cell type, electromagnetic and hadron calorimetry (CAL) with tile-fibre structure inside a super-conducting magnet coil. Finally several layers of muon detector surround the magnet coil. This detector has the expected performance much better than that

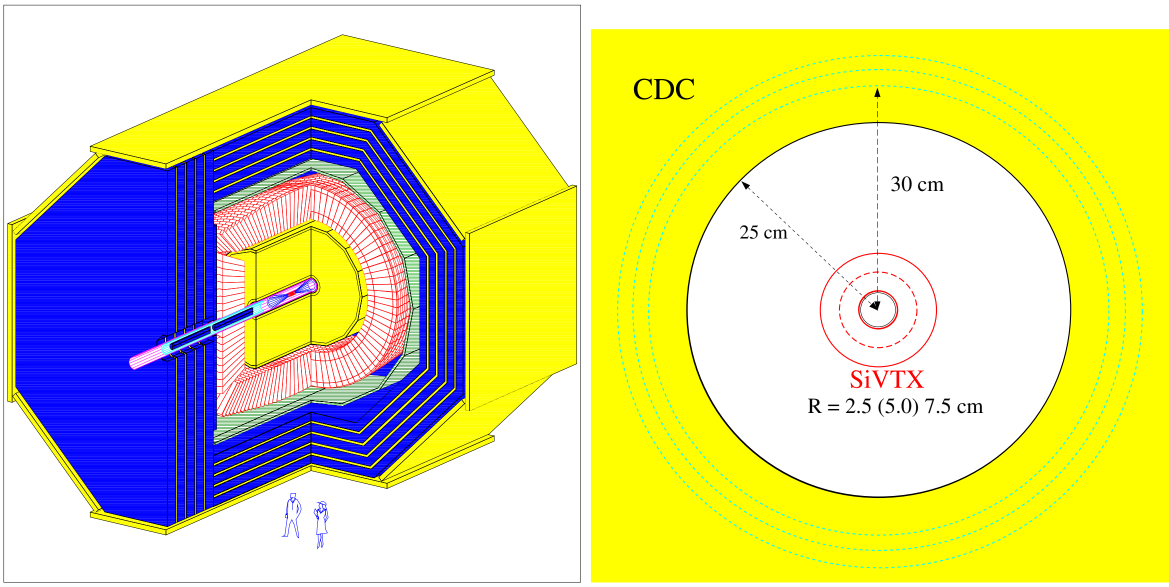

Figure 12: JLC-I model detector

of the existing detectors at LEP, and expected to satisfy the most of the requirements of the Higgs measurements we wish. Table 3 shows the performance expected for JLC-I detector compared to the OPAL detector at LEP.

Figure 13 shows the performances expected with the JLC-I detector with simulations. The upper-left plot shows the expected impact parameter resolution with track fitting. The upper-right plot shows the results obtained for the impact parameter resolution for cases of two and three layers of SI-VDET. The improvement from the increased number of layers and thinner material of the detector can be seen. The distributions of the obtained normalised impact parameter, impact paramter devided by the expected resolution, are shown in the bottom-left plot. In the plot, the distributions for the tracks from the b-hadrons decay in the Higgs event and those from the charm hadron in the W-decay are seen, together with the distribution for the tracks produced at the primary vertex. These results are made with a simple smearing process of the hit position in the SI-VDET and CDC with the expected

OPAL		JLC-I (Sep. 1998)
0.435 T	Magnetic Field	2.0 T
	Si vertex detector	
Double sided strip	detector type	CCD-pixel
2	number of layers	3
5.5 cm, 7.5 cm	radius	2.5, 5.0, 7.5 cm
$\lvert\cos\theta\rvert < 0.9$	Si Acceptance	$\lvert\cos\theta\rvert < 0.9$
18 (24) μm in r-ϕ (z)	IP resolution (50 GeV)	< 10 μm in r-ϕ and z
	Central chamber	
Large Jet-chamber	detector type	Small-cell Jet-chamber
$1.25 \cdot 10^{-3} \cdot p_{\mathrm{t}}$ (GeV)	$\sigma p_{\mathrm{t}}/p_{\mathrm{t}}$	$5 \cdot 10^{-5} \cdot p_{\mathrm{t}}$ (GeV)
135 μm	σx/wire in CDC	100 μm
~ 20 mm	σz/wire in CDC	< 2 mm (with stereo wire)
	Calorimeter	
Lead Glass	Electromagnetic Cal.	Tile fibre
7 % $/\sqrt{\mathrm{E}\ (GeV)}$	σE/E (γ, e)	14 % $/\sqrt{\mathrm{E}\ (GeV)}$
Fe+Streamer tube	Hadron Cal.	Tile fibre
120 % $/\sqrt{\mathrm{E}\ (GeV)}$	σE/E (hadron)	40 % $/\sqrt{\mathrm{E}\ (GeV)}$
	Forward Detectors	
Down to 25 mrad	Acceptance	$\lvert\cos\theta\rvert < 0.99$ for CAL.

Table 3: Performance expected for the JLC-I model detector in the present design. The left raw shows that of the OPAL detector at LEP to be compared.

material effect and the intrinsic resolution of the detector. Note that the track fitting has been made with the correct association of the hits, hence no effects of the mis-assignment of the hits are included. In this mannar, several preliminary physics studies have been made. One of the example is shown in the bottom-right plot, which shows the results obtained by I. Nakamura and K. Kawagoe for the branching ratio measurement of $\mathrm{Br}(\mathrm{h}^0 \rightarrow \mathrm{c\bar{c}} + gg)/\mathrm{Br}(\mathrm{h}^0 \rightarrow \mathrm{b\bar{b}})$ taken from Ref. [14].

7 Machine-Related Effects

In order to achieve the precise measurements, high luminosity of more than 5×10^{33} cm^{-2}s^{-1} is required at JLC, which is about 2 order higher than that at LEP running now. The extremely high luminosity and the beam structure necessary for the high gradient acceleration in the linear collider cause different experimental situation compared to LEP/SLC, i.e. larger machine related background and degradation of the beam momentum. There are two major machine related backgrounds in addition to the physics background at JLC. One is the huge number of background hits in the vertex detector due to large number of low energy $\mathrm{e}^+\mathrm{e}^-$ pairs created by beam-beam interaction (see Ref. [16]). Another is the overlap of two or more physics event due to high luminosity per bunch. One more big difference between LEP/SLC and JLC is the energy spread of the beam at the $\mathrm{e}^+\mathrm{e}^-$ interaction due to beam-strahlung effect [16].

7.1 Noise hits on Vertex Detector due to Beam-beam interaction

Fig. 14 shows the beam structure expected at JLC. The beam has bunch structure, 50 to 100 of which are grouped into train. The bunch spacing of 1.4 to 5.6 nsec is expected and the number of train per second (repetition rate) is designed to be 50–150 Hz. The readout scheme of the SI-VDET can be found in Ref [17].

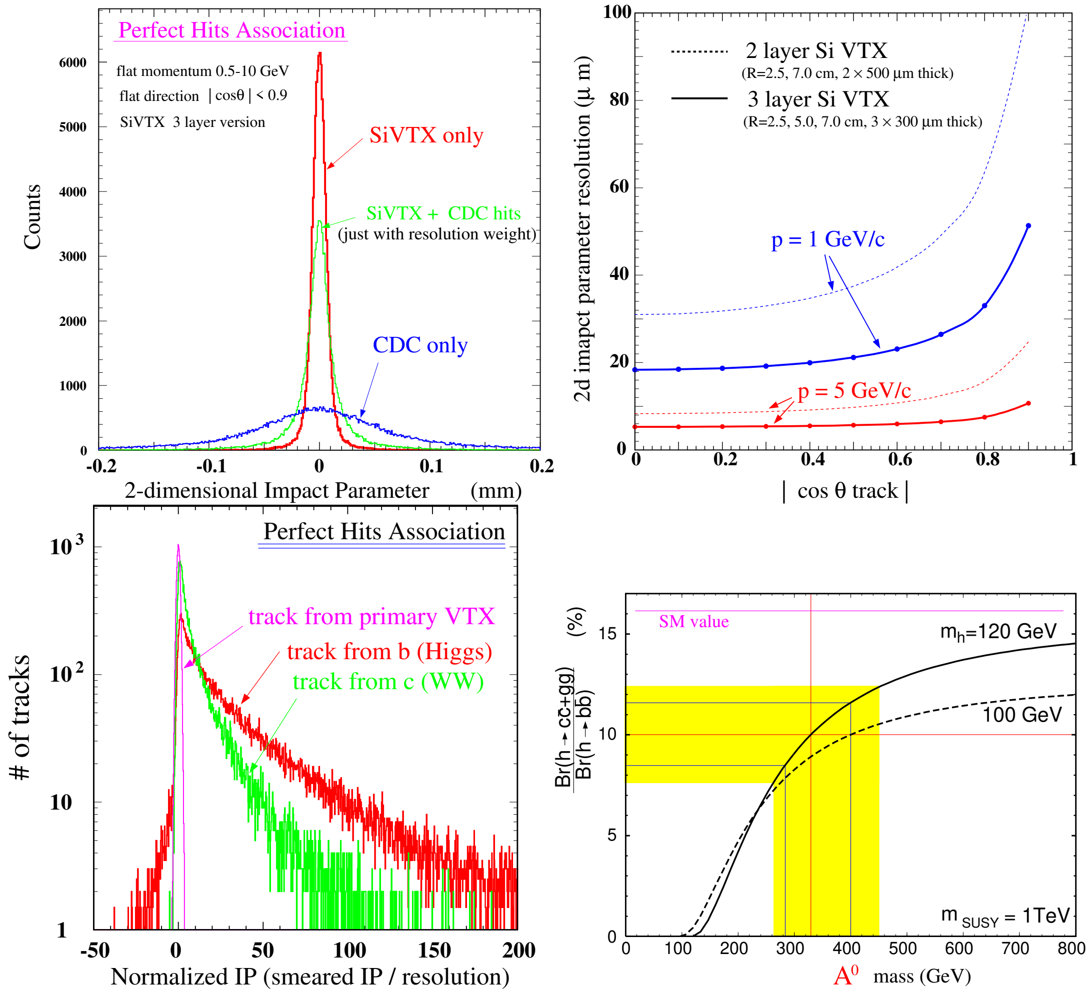

Figure 13: Performances obtaind in the smearing simulation (see the text). The bottom-right plot is taken from Ref. [14].

Since present design uses CCD readout for SI-VDET, the hits from multi bunches in a train overlap each other. In a single train collision, the expected rate of the noise hits due to the beam-beam interaction is about 100 hits per cm^2 on the inner most layer of SI-VDET. Note that the hits on a layer and the next layer can be highly correlated since the hits are induced by an electron (positron) from vicinity of interaction point of the beams.

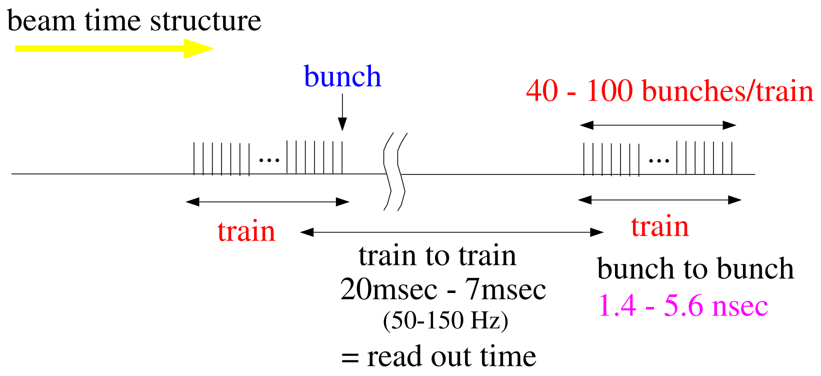

Figure 14: Time structure of the beam at JLC

The noise hits on the SI-VDET makes degradation of the performance of the vertex tagging for heavy flavours. Our experiences at LEP tell us the primary performance of the vertexing is determined by the mis-association of the hits in vertex detector to tracks observed in central chamber system, rather than the resolution of the vertex detector itself. In order to know the effect of the noise hits due to the beam-beam interaction for the vertexing, J. Kanzaki has performed a simulation of tracking of a particle with the noise hits. The simulation has been performed with full simulation code JIM [18] of JLC-I detector. The JIM simulator is written by J. Kanzaki, Y. Fujii, Y. Sugimoto, T. Tauchi et al, based on GEANT3. ABEL [19] program written by K. Yokoya and T. Tauchi has been used to simulate the creation of the e^+e^- pairs and γ's, with a set of machine parameters expected at JLC. Single track of muon as a signal is produced from the beam interaction point, and processed through the full simulation JIM, together with numbers of e^+e^- and γ's generated by ABEL. Three layers of SI-VDET are put at radius of 2.5, 5.0 and 7.5 cm from the beam axis. The most inner layer of the CDC are set at radius of about 30 cm. The magnetic field of 2 Tesla has been used for the simulation. The position resolution of the hits in SI-VDET are assumed to be about 7 μm, and 100 μm for the CDC. Resulting hits in the detector are reconstructed to a track. The process starts from tracking of the hits in CDC, then search for the corresponding hits in SI-VDET, and re-fit these. Note that the tracking program is not fully optimised for the JLC environment. Table 4 shows the results of the simulation. The fractions of the "good" tracking are seen for various momentum of the signal (muon) track. The reconstructed tracks are labelled as "good" when the impact parameter of the track, extrapolating to the production point, is found to be smaller than about two times the resolution for case without noise hits. For tracks with momentum more than 5 GeV/c, the effect of the noise hits can be neglected. However, for the lower momentum where the most of the tracks from b-hadron coming from Higgs signal are, the degradation of the impact parameter due to the mis-association is significant. This is mainly because of large multiple-scattering of the particle in CDC inner window and the large distance between the most inner layer in CDC and SI-VDET, which is more than 20 cm.

Track Momentum	Good track rate (Wrong hit rate) (%)	
(GeV)	(A) no bkg.	(B) with noise hits
0.5	91.0	21.5 (55.2)
1.0	90.3	87.7 (5.8)
2.0	91.3	90.8 (2.2)
5.0	92.1	92.1 (0.7)
10.0	89.5	89.5 (0.5)
20.0	90.4	90.4 (0.2)

Table 4: The rate of the "good" track reconstruction obtained in the full simulation with current JLC-I model detector for single muon. The "good" tracking is defined for tracks having the impact parameter (IP), with respect to the production point of the muon, to be less than about 2 σ of the IP resolution for the case with no background. (A) is for the case there are no background, which just represents the track finding efficiency with cut at about 2 σ resolution. (B) is for the rate obtained with the additional background hits due to the beam-beam interaction (see the text). In parentheses shown are the rates of the track reconstructed with at least one wrong hits associated in the track finding.

We have a lot of rooms to improve the performance of the association of hits. For example;

1. Increase the number of layers of SI-VDET from 3 to 4 or more.
2. Insert layers of an Intermediate Tracker (IT) between SI-VDET and CDC.
3. Reject apparent noise hits on SI-VDET using the cluster shape analysis, which is proposed by Y. Sugimoto.
4. Code more optimised and sophisticated tracking program.

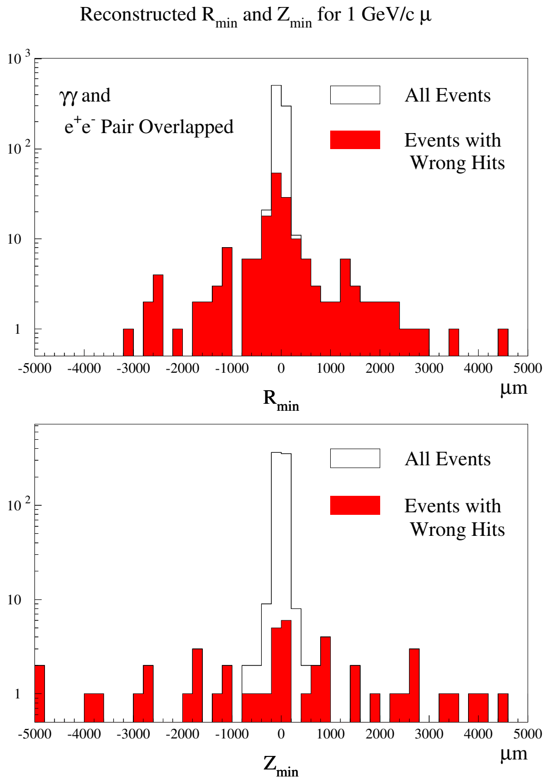

Figure 15: Distributions of the reconstructed impact parameter for 1 GeV/c muon in the full simulation with JLC-I model detector. The expected noise hits due to the beam-beam interaction and two-photon process are overlaied on the vertex detector in the simulation. The empty histograms show the distributions with correct assignment of the hits for the muon track. The hatched histograms are for those with at least one noise hits wrongly associated to the track.

In order to perform a good tracking, a self-fit capability in SI-VDET is very helpful. The IT in the second item should also very helpful to extrapolate the CDC track to SI-VDET. We expect the IT does not have to have resolution similar to SI-VDET. For the purpose of the extrapolation, we think the resolution of 20 μm is enough for the detector. The IT region has negligible hits due to beam-beam interaction, since almost e^+e^-'s from that are of low momenta, and be swept out by the magnetic field. The occupancy is low enough. Hence one of the possible detector might be Si-strip detector. Of course the additional timing information of the IT, if possible ($<$ 30 nsec), is highly welcome. In this workshop we have heard that the inner radius of the CDC might be enlarged to 40 cm or more [20] because of the new support tube system. In the case, the role of the IT becomes more important. For the third item, the cluster shape analyses has been done by I. Ueda after this workshop. He made his own clustering program, and the resulting clusters are checked with a simple filter program with information of number of pixels in a given cluster and width of the cluster. Table 5 shows the results of the cluster shape analyses. About 2/3 of the noise hits can be rejected while the signal hits are kept with more than 95 % efficiency.

Signal Hits (μ)			Noise Hits		
Layer 1	Layer 2	Layer 3	Layer 1	Layer 2	Layer 3
98.5 %	98.0 %	96.2 %	36.9 %	42.3 %	35.5 %

Table 5: The selection efficiency of the cluster finding with the cluster shape analyses to reduce the noise hits due to the beam-beam interaction.

7.2 Overlap of Physics Events

It is extremely difficult to separate events occurred in one bunch collision. The events are produced in too short time to separate these with timing information of hits observed in detectors such as CDC or CAL. Only possibility is the separation of events for charged tracks. When we have the beam spread wide enough, the tracks originating from one event and another can be distinguished when we see the separated two primary vertex positions. However, for neutral particles such as γ and K_L^0, the method can not work. Furthermore, the displaced vertex is the one of the signature of the b or c-hadron. Hence the rejection of the tracks from displaced vertex might make significant bias in the Higgs Br measurements. This kind of background has been negligible at LEP/SLC. Now it becomes problematic at the future linear collider, since the integrated luminosity in a bunch (luminosity per bunch) is expected to be large enough to observe such phenominon. The luminosities per bunch are about 10^{-3} μb^{-1} at LEP and about 10^{-2} μb^{-1} at SLC. At JLC, the luminosity per bunch can reach up to 1 μb^{-1} level, which is 2–3 order of magnitude higher than that at LEP/SLC. The most sever overlap comes from two-photon background. The detail of the two-photon background at JLC can be found in Ref. [21]. Note that the two-photon process include "normal" two-photon process in which the two virtual photon interacts, and interaction between a virtual photon and real photon induced by the beam-strahlung effect, which roughly doubles the cross-section. There are about factor two ambiguity of the production cross-section for the two-photon process. And it does depend on the kinematic cuts to define the process. Roughly speaking, the cross-section is around 100 nb. For simplicity, let us assume two-photon cross-section of 200 nb, the luminosity per bunch of 1 μb^{-1}, and also assume that we have perfect identification of the bunch of the event (no overlap with events in the side bunch). In this case, the two-photon process happens in 20 % of the bunches in average. The assumption of the perfect bunch identification may have to be relaxed when we have short bunch spacing of 1.4 nsec. When we have time resolution of the events corresponding to ±1 bunch, the overlap rate is 3 times higher, in which case more than half bunches contain two-photon events. In the extreme condition, most of the signal events, as well as the background process from hard interaction such as W^+W^-, Z^0Z^0 or $q\bar{q}$ production, are observed overlapping with such two-photon background. The effective cross-section σ_{eff} of the overlapping events can be written as $\sigma_{eff} = \sigma_1 \times \sigma_2 \times \mathcal{L}_{bunch}$, where $\sigma_{1,2}$ are the production cross-section of the single physics process, and $\mathcal{L}_{bunch}$ is the luminosity per bunch. Note that it has to be modified with Poisson probability for only one two-photon overlap, two two-photon overlap, three or more etc.. for large overlapping rate.

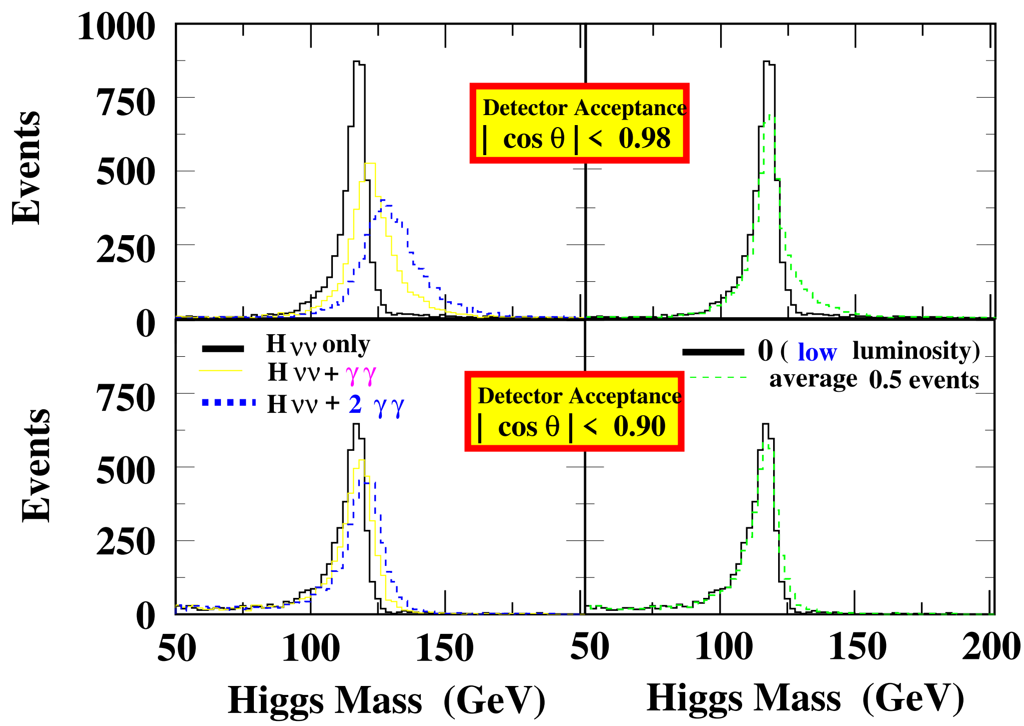

Figure 16: Distributions of the reconstructed mass of the Higgs in $e^+e^- \to \nu\bar{\nu}h^0$ process. Upper plots are for the mass with hits observed in the detector acceptance $|\cos\theta| < 0.98$, and bottom plots are for $|\cos\theta| < 0.90$. Left plots are those for none, one, two two-photon events overlapped with the signal events. The dotted lines in the right side plots are the reconstructed mass in case 0.5 events are expected in average for the overlap rate.

There are two major effects in the measurements. One is the effect on the kinematics such as reconstructed mass of the Higgs and the selection bias in the Higgs hunt. The additional energy from the two-photon overlap makes strong distortion of the reconstructed mass, especially in the $e^+e^- \to \nu\bar{\nu}h^0$ process. Also new event topologies are introduced in the background process, which might leads large bias and less performance in the event selection. The other effect is that in the flavour tagging which relies on the tracks displaced from the event primary vertex. The overlapping event has, in general, its event-production-point different from the original event, since the beam has a finite width. If we use the information only in r-ϕ projection, the effect can be minimised thanks to the tiny width of the beam in the projection. However the beam spread is larger in the beam-direction.

Several simulation studies has been started. The simulation overlaps the hard scatering events of signal or background processes, with one or more two-photon process. We have used the JSF Quick-simulator [22] made by A. Miyamoto. The data base separately generated for the hard processes and the two-photon background are overlapped afterwards. Figure 16 shows the reconstructed mass of the Higgs for the $e^+e^- \to \nu\bar{\nu}h^0$ process with/without two-photon overlap. The reconstructed mass is shown for the different detector accepatance to be used in the calculation. Since the two-photon background tends to make energy-flow in the forward region, the bias in the mass reconstuction can be reduced if we use the detector information only for the central part, while the signal tagging efficiency in a mass window is reduced. Simulation studies have been made also for the flavour tagging. Possible bias has been checked with different assumptions for the beam spread in beam direction. As we have expected, the effects are found to be negligible in r-ϕ projection. The results obtained in the simulation studies in the 3-dimensional tagging show a significant bias if the beam spread is about 400 μm or more in the beam direction. The effect is much smaller for the case with 80 μm which is the currect value for JLC.

7.3 Beam-strahlung

The beam-strahlung cause the spread of the e^+e^- centre-of-mass energy. This makes distortion of the reconstructed Higgs mass as well as the background process.

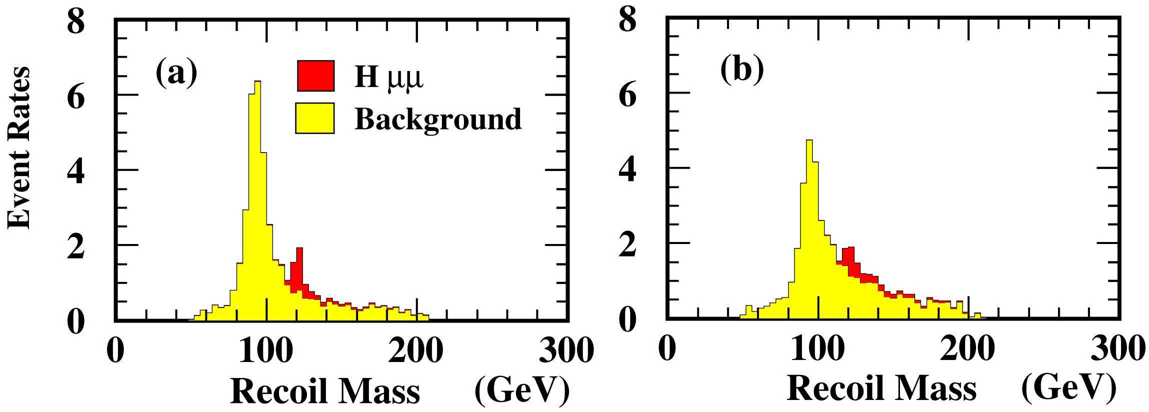

Figure 17: Distributions of the recoil mass for signal (black hatched histogram) process of $e^+e^- \to h^0Z^0 \to h^0\mu^+\mu^-$ with h^0 mass of 120 GeV, and the background process mainly from Z^0 pair production (grey histogram) (a) for the case without beam-strahlung effect at $\sqrt{s} = 300$ GeV, and (b) for the case in which the beamstrahlung is considered in the production. The beam parameters for $\sqrt{s} = 500$ GeV mode are used in the simulation. For parameters of 300 GeV setting, the situation would be better.

We have discussed the leptonic channels $e^+e^- \to Z^0h^0 \to \ell\ell X$ (ℓ=e or μ) can provide the Higgs boson production cross-section independently of its decay branch, using the recoil mass information. However the recoil mass distribution can strongly be affected by the beam-strahlung effect. As an example, the reconstructed mass of the Higgs in muon channel with/without the beam-strahlung effect are shown in Fig. 17. The beam-strahlung effect is simulated by the code provided by N. Tohmi et al. One may improve the reconstructed mass spectrum with a convolution of the beam-strahlung effect in its calculation of the mass. The improvement is the subject in the next step.

8 Summary and discussion

The study of the Higgs boson is the key to open the future generation of the particle physics. It has great possibility to let us know the fundamental structure of the interaction of particles up to GUT scale or Plank scale. Even only with the Higgs mass determined by future experiments, we might be able to select the models in various theories. In order to establish the Higgs mechanism and determine the coupling between Higgs and particles, precise measurements of the Higgs production and its decay are essential, which can be done only with the future e^+e^- linear collider. JLC gives us the great opportunity to proceed to the next paradigm. The possible mass regions of the lightest Higgs boson differ, model by model. There are, however, strong indication that the mass is lower than 300 GeV where the first phase of JLC covers well. When we assume MSSM, the mass is limited to be lower than 150 GeV. In NMSSM, the upper bound is about 140 GeV assuming the finite Higgs coupling up to GUT scale, and also in more general scheme the bound does not exceed 210 GeV. The indirect measurement of the electro-weak parameters at LEP/SLC/Tevatron give us upper bound of the SM Higgs mass of 230 GeV at 95 % CL. There always exist the lower limit of the production cross-section. Hence the discovery of at least one Higgs is guaranteed if our understanding of the nature is not so bad. One can say, in other words, it is really a "big discovery" when we find no Higgs at the first phase of the JLC. The experiment should start from lower energy, since the cross-section decrease with centre-of-mass energy. And if the Higgs is lighter than 250 GeV, we should operate the machine below the top-quark production threshold to avoid the top quark background which contains W and heavy flavours in the final state.

The decay branching (Br) of the Higgs depends strongly on the Higgs mass, since the coupling to W is strong enough to dominate the branching when the Higgs mass close to or above 160 GeV where real W^+W^- decay is kinematically open. For Higgs bosons with mass of lower than 140 GeV, the dominant decay mode is expected to be $b\bar{b}$ in most of the cases. Since the strong mass dependence of the branching ratio, the precise measurement of the Higgs boson mass with an accuracy of 100 MeV is needed, in order to translate the results of the Br-measurement to Yukawa-coupling strength so on. The Br-measurements can provide us the absolute strength of the couplings of Higgs with fermions and gauge bosons, in combination with the Higgs production cross-section measurements. There are a lot of Br measurement. The most interesting measurements are the Br measurement of $b\bar{b}$, $\tau^+\tau^-$ and W^+W^-. When we combine the $Br(h^0 \to W^+W^-)$ with the cross-section measurement, the total width of the Higgs can be deduced. The $Br(h^0 \to \tau^+\tau^-)/Br(h^0 \to b\bar{b})$ measurement is also the one of the essential measurements. This might prove/exclude the type-II coupling, which is commonly assumed in the SM or MSSM, of the Higgs to quarks and leptons. On the other hand, assuming the coupling of type-II, the measurement serve as the precise measurement of the running b-quark mass at the Higgs mass. There are also other important channels to be measured. For instance, $Br(h^0 \to c\bar{c})/Br(h^0 \to b\bar{b})$, $Br(h^0 \to gg)/Br(h^0 \to b\bar{b})$ or $Br(h^0 \to c\bar{c}+gg)/Br(h^0 \to b\bar{b})$ has large discrimination power of MSSM from SM. The ratios are sensitive to A^0 mass in MSSM, with little dependence on other SUSY parameters such as scalar top mass. However, the current theoretical ambiguity due to uncertainty of the c-quark mass and α_s is still large. Theoretical improvements are awaited for.

The Higgs discovery is easy at JLC. This is demonstrated with the existing full simulation of the OPAL detector at LEP. We need only one day running to discover Higgs, which is extremely different situation from other experiments such as at LHC. However our purpose of the experiment is not only the discovery. For the precise measurement, we need a detector(s) with the performance much better than those of the experiments presently running. The key points of the Higgs measurements are good energy resolution or particles and jets, accurate vertexing performance for the flavour tagging, and particle identification especially for tau-lepton. Studies of the performance of the measurements has been started with JLC-I detector as a model detector. Preliminary results indicate that the Br-measurement with accuracies of 2–10 % for $\mathrm{Br}(\mathrm{h}^0 \to \mathrm{b}\bar{\mathrm{b}})$, $\mathrm{Br}(\mathrm{h}^0 \to \tau^+\tau^-)$ and $\mathrm{Br}(\mathrm{h}^0 \to \mathrm{W}^+\mathrm{W}^-)$ with 1–3 years running at JLC. Note that the errors are statistical only, and simulated with fast simulator without machine related background, and the analyses are still in very preliminary stage.

We have also started the full simulation studies in an expected situation including large backgrounds related to the acceleration scheme and extremely high luminosity. The main differences between LEP/SLC and coming JLC in the experimental condition are 1) the huge hits in vertex detector due to beam-beam interaction, 2) the possible high rate overlap of background events, especially the two-photon process, on the signal events as well as on the other had scattering background processes, and 3) the large beam momentum spread due to beam-strahlung. Some of the results obtained in the preliminary studies has been presented. It turned out that the Higgs measurements are not that so easy when we consider such machine related effects. The first important consequences of the studies are on the bunch identification capability of the trackers and calorimetry. We need to have time resolution shorter than 1 nsec level for calorimeters and similar for the central tracker with self-fitting. For central tracker, the stereo wire might need to be optimised also with this sense. These are required to minimise the effect of the overlap of events from other bunches. In order to reduce the mis-association of hits on vertex detector and CDC tracks, several possible modification has been discussed. One is to insert several layers of intermediated tracker in the large area between CCD vertex detector and central gas chamber. The increased number of layers for the vertex detector should be helpful. And in software side, more optimised algorithm is indispensable. As we have discussed, there are still a lot of things to do by the construction of the linear collider.

We hope we start the experiment as soon as possible, to determine the direction of the next generation of the particle physics.

Acknowledgements

First of all, we would like to express our sincere gratitude to Prof. Yu-Ping Kuang for the host of the first ACFA workshop on the physics/detector at linear collider at Tsinghua University, Beijing, the People's Republic of China. We also would like to express our special thanks to organizers of the workshop, stuff members and students at Tsinghua University for the wonderful organization, supports and hospitality. Some of the important results presented in this document are obtained with combined efforts of many individuals with close collaboration. Especially, we wish to appreciate Dr. J. Kanzaki for the studies of the tracking with full simulation JIM. We also would like to thank Dr. I. Nakamura for the simulation with the OPAL detector codes, and Dr. I. Ueda for the cluster-shape analysis and studies of the beamstrahlung effects. We are also thankful to Prof. T. Tauchi for the various discussion on the beam-related backgrounds, two-photon process and generation of the $\mathrm{e}^+\mathrm{e}^-$ pairs due to beam-beam interaction, Dr. Y. Sugimoto for the various suggestions and new ideas for the vertex detectors and clustering, Prof. A. Miyamoto for the discussions on his quick simulators and coding of it, Dr. K. Fujii for the discussions of various physics aspects at JLC, Dr. Y. Fujii for the helpful discussions on the calorimeters, and Dr. N. Tohmi for the program to generate the beam momenta with the beam-strahlung. We sincerely thank Prof. T. Matsui for his leading the KEK JLC-group, and various encouraging predictions. Special thanks are given to Prof. S. Komamiya for continuous discussions, suggestions and encouragements in the whole aspects of the future $\mathrm{e}^+\mathrm{e}^-$ linear collider. We would like to stress our special thanks to Prof. S. Iwata for his huge efforts as the ACFA chairman, and also as the chief of the JLC promotion office at KEK. Finally, we thank all of the ACFA members and JLC group members.

References

[1] P.W. Higgs, Phys. Lett. **12** (1964) 132;
F. Englert and R. Brout, Phys. Rev. Lett. **13** (1964) 321;
G.S. Guralnik, C.R. Hagen, and T.W.B. Kibble, Phys. Rev. Lett. **13** (1964) 585.

[2] Chang-Gen Yang, *Recent results from LEP – Precision EW*, in these proceedings;
Atul Gurtu, *Recent results from LEP – New Particle Searches*, in these proceedings;
ALEPH Collaboration, R. Barate *et al.*, Phys. Lett. **B440** (1998) 419;
DELPHI Collaboration, P. Abreu *et al.*, CERN-EP/99-06, to be published in Eur. Phys. J. **C**;
L3 Collaboration, M. Acciarri *et al.*, Phys. Lett. **B436** (1998) 389;
OPAL Collaboration, G. Abbiendi *et al.*, Eur. Phys. J. **C7** (1999) 407;
ALEPH, DELPHI, L3, and OPAL collab., and the LEP Working Group for Higgs Boson Searches, CERN-EP/99-060.

[3] Sun Kee Kim, *Recent results from Tevatron*, in these proceedings.

[4] See for example; M. Carena, *et al.*, CERN-TH-99-203, Jul 1999. 35;
S. Abdullin *et al.*, Phys. Lett. **B431** (1998) 410;
S. Moretti, CAVENDISH-HEP-95-18, Nov 1996. 52, hep-ph/9612310, and their references.

[5] See for example; N. Akasaka *et al.*, *JLC DESIGN STUDY*, KEK-REPORT-97-1 (1997) 617;
JLC Group, **JLC-I** (the green book), KEK-REPORT-92-16 (1992);
Web page *http://www-jlc.kek.jp/*

[6] Y. Okada, M. Yamaguchi, T. Yanagida, Phys. Lett. **B262** (1991) 54.

[7] J. Kamoshita, Y. Okada, M. Tanaka, Phys. Lett. **B328** (1994) 67;
T. Moroi, Y. Okada, Phys. Lett. **B295** (1992) 73.

[8] J.R. Espinosa, M. Quiros, Phys. Rev. Lett. **81** (1998) 516.

[9] *HIGGS PHYSICS AT LEP-2*, in CERN LEP-2 yellow report vol.1, CERN-96-01.
W. Kilian, M. Kramer, P.M. Zerwas, Phys. Lett. **B373** (1996) 135.

[10] T. Omori, *A Polarized Positron Beam for Linear Collider*, KEK-PREPRINT-98-237, 1999. (in these proceedings).

[11] T. Omori, Y. Kurihara, Y. Sugimoto, Y. Fujii, K. Fujii, KEK-Proc.-94-01, 102-111.
T. Omori, Proceedings of LCWS93, Waikoloa, Hawaii (1993) 791.

[12] J. Kamoshita, Y. Okada, M. Tanaka, Phys. Lett. **B391** (1997) 124.

[13] M.D. Hildreth *et al.*, Phys. Rev. **D 49** (1994) 3441

[14] I. Nakamura and K. Kawagoe, Phys. Rev. **D 54** (1996) 3634.

[15] See for example; T. Tauchi, *Detector Overview*, in these proceedings.

[16] K. Yokoya and P. Chen, *Beam-beam phenomena in linear colliders*, Frontiers of Particle Beams: Intensity Limitations, edited by M.Month and S.Turner, Lecture Notes in Physics Vol. 400, 415-445;
T. Tauchi, K. Yokoya and P. Chen, *Pair creation from beam-beam interaction in linear colliders*, Particle Accerelators, 1993, Vol.41, 29-39.

[17] Y. Sugimoto, *Vertex Detector at JLC*, in these proceedings;
Web page; *http://acfahep.kek.jp/subg/vtx/*;
H. Yamamoto, *Pixel Detectors*, in these proceedings.

[18] Web page; *http://www-jlc.kek.jp/subg/offl/jim/index-e.html*

[19] K. Yokoya and T. Tauchi, *ABEL* (Analysis of Beam-beam Effects in Linear colliders) program.

[20] Norik Khalatyan, *Central Tracker*, in these proceedings.

[21] T. Tauchi and H. Hayashii, Proceedings of LCWS93, Waikoloa, Hawaii, 26-30 April 1993, p745, KEK-preprint 93-105.

[22] A. Miyamoto, *JSF*, in these proceedings.
Web page; *http://acfahep.kek.jp/subg/sim/*